Synthesis of iron oxide nanoparticles in a microfluidic device: preliminary results in a coaxial flow millichannel†

Ali Abou Hassan,*[a] Olivier Sandre,[a] Valérie Cabuil[a] and Patrick Tabeling[b]

Received (in Cambridge, UK) 19th December 2007, Accepted 24th January 2008
First published as an Advance Article on the web 18th February 2008
DOI: 10.1039/b719550h

A millimetric coaxial flow device operating under laminar flow has been designed to study the synthesis of iron oxide nanoparticles in a millichannel where the flow rate of the different reagents has been adjusted all over the experiments so that the magnetic and stable colloidal iron oxide particles with a size less than 7 nm have been prepared continuously.

Miniaturization of chemical reactions and the development of "lab on a chip" (LOC) technology has gained significant importance in the recent years.[1] One predicts indeed that small dimensions of vessels lowers the diffusion times of chemical species, so that mass transport is improved in microstructured reactors.[2] Scaling down reactor dimensions is proposed as an opportunity to improve size and composition control in the field of materials synthesis.[3] Local variations in reaction conditions such as concentration and temperature are minimized and therefore control of both nucleation and particle growth can be used to improve monodispersity in nanoparticles synthesis.[4]

As an example, the synthesis of iron oxide nanoparticles has attracted much attention, motivated by their wide range of applications. Colloidal iron oxides are used as single bit-elements in high density magnetic data storage arrays,[5] ionic ferrofluids,[6] and in the biomedical field, for example as contrast enhancement agents for Magnetic Resonance Imaging,[7] or for hyperthermia,[8] *etc.*... Because the properties of these nanocrystals strongly depend on their dimensions, the synthesis of monodisperse nanoparticles is one of the most challenging problems. At the beginning of the 1950's V. K. Lamer and R. H. Dinegar proposed a mechanism based on a nucleation-growth process to describe the synthesis of nanoparticles.[9] Since then, various chemical synthetic strategies have been reported to obtain monodisperse nanoparticles with different shapes.[10] Recently, several groups designed microreactors and reported the improvement of inorganic and metallic nanoparticles synthesis. However, the synthesis of inorganic materials has been focused on Quantum Dots such as CdS[11] or CdSe,[12] silica,[13] titania,[14] and silica–titania core-shell colloidal nanoparticles.[15] There has been until now no reported study of the synthesis in microchannels of colloidal iron oxide nanoparticles from the following alkaline coprecipitation reaction:

$$Fe^{2+}_{(aq)} + 2\ Fe^{3+}_{(aq)} + 8\ OH^{-}_{(aq)} \rightarrow Fe_3O_{4(s)} + 4\ H_2O_{(l)}$$

Preliminary tests of this co-precipitation reaction in typical Y-shaped microreactors led to the clogging of the channel by a precipitate sticking to the glass cover-slip. In order to isolate the nanoparticles from the walls, we designed a 3D millifluidic device performing the mixing of two coaxial flows of miscible fluids (Fig. 1), one containing the iron "precursor salts", the other a strong base. The length of the capillary from the confluence region to the outlet is 3 cm. A (poly)tetrafluoroethylene (PTFE) tube (500 μm ID and 10 cm long) leading to a sample vial was connected to the reactor outlet. Depending on the two flow rates Q_{in} and Q_{out}, the residence times range between 10 and 48 s. The outer capillary with a 1.7 mm diameter (*d*) was shaped by the molding of cylindrical tubing (Upchurch Scientific) in a Petri dish with polydimethyl siloxane (PDMS, Sylgard 184) and subsequent removal when the resin was cured. The central capillary with 150 μm of inner diameter (ID), 360 μm of outer diameter (OD) was obtained by fixing a glass capillary (Plymicro®, usually used for Capillary Electrophoresis) inside the tip of a micropipette (Gilson), whose conical shape enables a precise centering. By comparison with a 2D flow focusing device (*i.e.* a typical "Y-shaped"

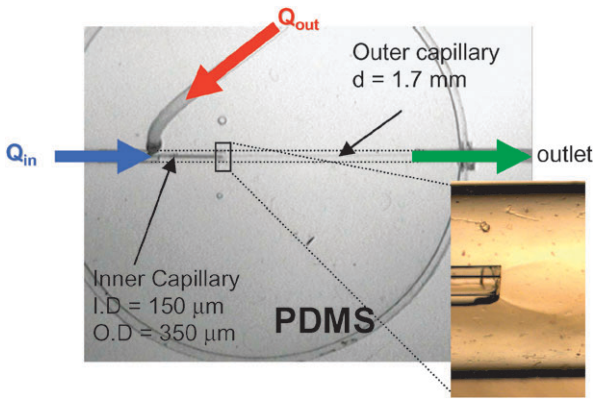

Fig. 1 A coaxial flow device operating under a laminar regime. The inset image shows the outlet of the inner capillary with the solution of iron II and iron III flowing into the stream of TMAOH alkaline solution.

[a] *Laboratoire Liquides Ioniques et Interfaces Chargées (LI2C), UMR7612 UPMC Univ Paris 06/CNRS/ESPCI, Université Pierre et Marie Curie, 4 place Jussieu, case 51 75252 Paris cedex 5, France. E-mail: abouhas@ccr.jussieu.fr; Fax: +33 (1) 44273228; Tel: +33 (1) 44273166*
[b] *Laboratoire "Microfluidics, MEMS & Nanostructures" (MMN), UMR7083 CNRS/ESPCI, Ecole Supérieure de Physique et de Chimie Industrielles de Paris, 10 rue Vauquelin 75231 Paris cedex 5, France*

† Electronic supplementary information (ESI) available: COMSOL Multiphysics® simulations and focusing/defocusing images. See DOI: 10.1039/b719550h

channel), the 3D coaxial flow's setup offers two main advantages: on the one hand, it enables a precision positioning of the "precursors" flow at the centre of the channel in both longitudinal and lateral dimensions and on the other hand it avoids adsorption of any precipitate species onto the PDMS walls, which are totally wetted by the alkaline outer flow.

A solution of total iron salts concentration $c = 10^{-2}$ mol L^{-1} with 0.5 as molar ratio Fe(II)/Fe(III) was prepared by mixing $FeCl_3$ and "fresh" $FeCl_2{\cdot}4H_2O$ salts in diluted and degased hydrochloric acid (pH $\sim$ 0.4). Diluted hydrochloric acid was used as Fe(II) ions are more stable in acidic media so non iron hydroxide can precipitate. The tetramethylammonium hydroxide ($(CH_3)_4NOH$, TMAOH) at a concentration of 0.172 mol L^{-1} was the alkaline solution. Both solutions were injected into the channel through two syringes actuated automatically (Harvard apparatus), the iron "precursors" solution was pumped into the inner capillary and the TMAOH base into the outer capillary of the channel. TMAOH was chosen prior to any other base as the TMA^+ cations afford enhanced stability of colloidal oxide dispersion.[16]

The volumetric rate flows of both solutions (respectively Q_{in} and Q_{out}) were adjusted to avoid any turbulent vortex in the capillary as described in the hydrodynamic study of co-axial flows by Andreev *et al.*[17] We observed experimentally the well-known transition between the focusing of the inner flow for large values of the ratio $Q_{out} : Q_{in}$ to de-focusing conditions for lower values (see ESI where the only difference compared to Fig. 1 is the inner diameter of the central capillary 50 μm instead of 150 μm†). We have also performed numerical simulations of the Navier–Stokes equations in axisymmetric geometry (available as ESI†) using the COMSOL Multiphysics® software. For our experiments, the defocusing of the stream offers the advantage of a larger surface area between the inner and outer solutions, which decreases the concentration of nanoparticles in the reaction space at neutral pH where they are unstable (yellow region in the graphical abstract) before reaching values of pH above the PZC where they are stabilized by their negative surface charge density.

Owing to the laminar regime in the channel, mixing is controlled by the diffusion of the species.[18] In the absence of shear flow, the molecular diffusion coefficients D° of iron complexes $[Fe(OH_2)_6]^{2/3+}$ in aqueous solution are much slower than the ones of hydroxide ions OH^- and of the protons H^+.[19,20] In a Poiseuille laminar flow such as in the cylindrical millichannel, the values of the diffusion coefficients are highly increased by the so called Aris-Taylor dipsersion effect.[21] The full simulation of the system with both convection and diffusion of all the species is out of the scope of this paper. Nevertheless, we can quantitatively expect that the diffusion of iron complexes from the central acidic stream flow remains slower than the fast diffusion of H^+ and OH^-. As a result the local pH varies continuously from acidic in the central flow to basic at the periphery, the pH gradient being progressively smoothed out when moving towards the outlet of the channel. The coprecipitation reaction will therefore be likely confined in the neutral region at the interface between the two streams. The excess of TMAOH will allow the dispersion of the particles after their synthesis, and avoid their adsorption onto the walls. The particles will be collected at the outlet without any problem of plugging.

In order to stabilize the inner flow of the iron solution before initiating the hydrolysis, we injected at first a HCl solution of the same pH $\sim$ 0.4 in the outer stream. The outer flow is then switched to TMAOH solution. A few seconds after the outlet (time across the PTFE tubing), the reaction was "quenched" by fast solvant extraction to prevent any ageing of the nanoparticles in the aqueous solution. In practical, the collection vial containing a cationic surfactant didodecyldimethyl ammonium bromide ($C_{26}H_{56}BrN$, DDAB, $C = 0.02$ M) in cyclohexane was stirred at around 200 rpm with a glass helix stirrer.[22] A stable colloidal suspension of nanoparticles coated by DDAB is obtained in the cyclohexane phase.

Samples for Transmission Electron Microscopy (TEM) were prepared by placing a single drop of the resulting suspension onto a 200 mesh holey carbon-coated copper grid (SPI) which was then allowed to dry in air. The suspensions obtained by Fe(II)/Fe(III) coprecipitation were also analysed by Vibrating Sample Magnetometry (VSM).

As the flow of TMAOH was fixed ($Q_{out} = 400$ μl min^{-1}) and the volumetric flow of the iron precursors mixture was increased ($10 < Q_{in} < 100$ μl min^{-1}), the colour changed from brown to black, a characteristic of magnetite Fe_3O_4. The suspensions obtained in cyclohexane are always stable. However, Dynamic Light Scattering (DLS) measurements of the aqueous solutions showed that the colloidal suspension exhibits the lowest hydrodynamic size ($d_H = 120$ nm) for a value of $Q_{out}/Q_{in} \sim 4$. TEM observation of the colloidal suspension in cyclohexane indicated that the nanoparticles produced in the channel are fairly spherical with an average size around 7 nm. The evidence of their crystallinity is provided by the electron microdiffraction pattern in the inset of Fig. 2, which shows the presence of the maghemite phase γ-Fe_2O_3.

Although suspensions obtained in cyclohexane are stable in zero magnetic field, they precipitate in the presence of a magnetic field gradient (for example on a strong permanent magnet), which suggests a magnetic character. This

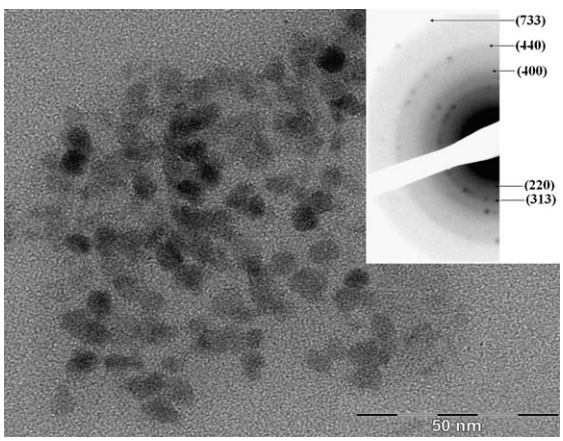

Fig. 2 TEM image of nanoparticles prepared in the channel (for flow rates $Q_{in} = 100$ μl min^{-1} and $Q_{out} = 400$ μl min^{-1}). The inset shows the electron microdiffraction pattern with the Miller indices of γ-Fe_2O_3.

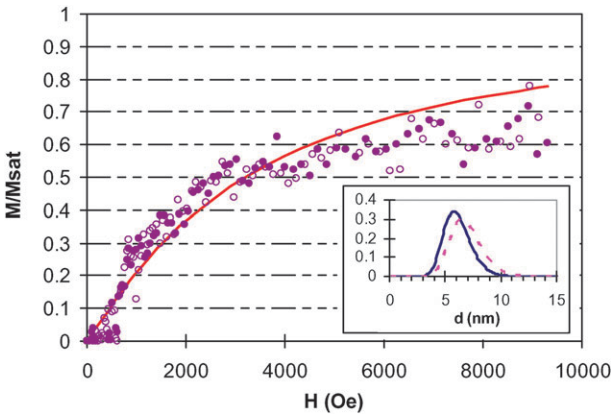

Fig. 3 Magnetisation curve of a stable suspension in water of nanoparticles produced in the millifluidic device. The inset curves represent the fitting Log-normal laws for the numbers distribution (solid line) and the volume distribution (dotted line) of diameters.

observation agrees with the VSM measurement on a stable unquenched (aqueous) suspension: the magnetization curve (Fig. 3) follows the Langevin law typical of superparamagnetism, calculated for an assembly of nanoparticles with a rather narrow distribution of diameters fitted by a Log-normal law of parameters $d_0 = 6$ nm and $\sigma = 0.2$. The particles' sizes deduced from the analysis of the magnetization curve shape are in good accordance with the TEM pictures. As was shown by Khan *et al.*[13] for the synthesis of silica nanoparticles in a millichannel, the Taylor-Aris dispersion effect in the flow of nanoparticles under growth induces a residence time distribution (RTD) which is responsible for their observed polydispersity of sizes. However, the relatively narrow size distribution obtained by our method ($\sigma = 0.2$) is below the typical values obtained by the batch coprecipiataion method ($\sigma = 0.35$).

By measuring both the volume fraction of nanoparticles $\phi = 5.7 \times 10^{-5}$ (from iron titration by atomic spectroscopy) and the saturation magnetization $M_{sat} = 7.9$ A m^{-1} for the suspension, we deduce a specific magnetization $m_s = M_{sat}/\phi = 1.4 \times 10^5$ A m^{-1} for the materials, which is below the bulk value of maghemite γ-Fe_2O_3 (3.5×10^5 A m^{-1}), but not far from the m_s value about 2.6×10^5 A m^{-1} usually obtained for nanoparticles of approximately the same sizes prepared with the standard large scale synthesis.[23] Therefore we can deduce that compared to classical ones, nanoparticles prepared within a few seconds in a millifluidic channel exhibit only a small decrease of ordering of their magnetic moments.

We have demonstrated that aqueous dispersions of superparamagnetic iron oxide nanoparticles can be prepared on chip in a millichannel reactor by providing a cylindrical geometry of the device and the use of TMAOH as alkaline reagent. These results open the way to other experiments such as online functionalization, online detection and the structural measurements of the nanoparticles. A further miniaturization of the channels would enhance the time resolution and enable kinetic studies of the coprecipitation mechanism.

We would like to thank Dr Hervé Willaime from "Microfluidics, MEMS & Nanostructures" (MMN) laboratory at ESPCI, France and Dr Caroline Derec, from "Matières et Systèmes Complexes" (MSC) laboratory at Univ. Paris 07, France for their very fruitful discussions at the beginning of this work. We thank also Patricia Beaunier from the Service de Microscopie Electronique de Paris 6 for TEM images.

Notes and references

1 M. Tokeshi, T. Minagawa, K. Uchiyama, A. Hibara, K. Sato, H. Hisamoto and T. Kitamori, *Anal. Chem.*, 2002, **74**, 1565.
2 K. Jaehnisch, V. Hessel, H. Loewe and M. Baerns, *Angew. Chem., Int. Ed.*, 2004, **43**, 406.
3 K. F. Jensen, *Chem. Eng. Sci.*, 2001, **56**, 293.
4 A. J. DeMello and J. C. DeMello, *Lab Chip*, 2004, **4**, 11N.
5 S. Sun and H. Zeng, *J. Am. Chem. Soc.*, 2002, **124**, 8204.
6 R. Massart, E. Dubois, V. Cabuil and E. Hasmonay, *J. Magn. Magn. Mater.*, 1995, 149; A. Bee, R. Massart and S. Neveu, *J. Magn. Magn. Mater.*, 1995, **149**, 6; O. Sandre, J. Browaeys, R. Perzynski, J. C. Bacri, V. Cabuil and R. E. Rosensweig, *Phys. Rev. E*, 1999, **59**, 1736.
7 M. S. Martina, J. P. Fortin, C. Menager, O. Clement, G. Barratt, C. Grabielle-Madelmont, F. Gazeau, V. Cabuil and S. Lesieur, *J. Am. Chem. Soc.*, 2005, **127**, 10676; W. J. M. Mulder, G. J. Strijkers, G. A. F. Van tilborg, A. W. Griffioen and K. Nicolay, *NMR Biomed.*, 2006, **19**, 142.
8 J. P. Fortin, C. Wilhelm, J. Servais, C. Menager, J. C. Bacri and F. Gazeau, *J. Am. Chem. Soc.*, 2007, **129**, 2628.
9 V. K. LaMer and R. H. Dinegar, *J. Am. Chem. Soc.*, 1950, **72**, 4847; V. K. LaMer, *Ind. Eng. Chem.*, 1952, **44**, 1270.
10 P. Jongnam, J. J. Soon, G. K. Youngjin and J. T. Hyeon, *Angew. Chem., Int. Ed.*, 2007, **46**, 4630.
11 J. B. Edel, R. Fortt, J. C. deMello and A. J. deMello, *Chem. Commun.*, 2002, 1136.
12 H. N. H. Wang, M. Uehara, Y. Yamaguchi, M. Miyazaki and H. Maeda, *Adv. Funct. Mater.*, 2005, **15**, 603; A. G. B. K. H. Yen, M. A. Schmidt, K. F. Jensen and M. G. Bawendi, *Angew. Chem., Int. Ed.*, 2005, **44**, 5349; H. Wang, X. Li, M. Uehara, Y. Yamaguchi, H. Nakamura, M. Miyazaki, H. Shimizu and H. Maeda, *Chem. Commun.*, 2004, 48; E. M. Chan, R. A. Mathies and A. P. Alivisatos, *Nano Lett.*, 2003, **3**, 199.
13 S. A. Khan, A. Gunther, M. A. Schmidt and K. F. Jensen, *Langmuir*, 2004, **20**, 8604.
14 H. Wang, H. Nakamura, M. Uehara, M. Miyazaki and H. Maeda, *Chem. Commun.*, 2002, 1462; B. F. Cottam, S. Krishnadasan, A. J. DeMello, J. C. DeMello and M. S. P. Shaffer, *Lab Chip*, 2007, **7**, 167.
15 S. A. Khan and K. F. Jensen, *Adv. Mater.*, 2007, **19**, 2556.
16 R. Massart and V. Cabuil, *J. Chim. Phys.*, 1987, **7**, 84.
17 V. P. Andreev, S. B. Koleshko, D. A. Holman, L. D. Scampavia and G. D. Christian, *Anal. Chem.*, 1999, **71**, 2199.
18 J. B. Knight, A. Vishwanath, J. P. Brody and R. H. Austin, *Phys. Rev. Lett.*, 1998, **80**, 3863.
19 According to the Stokes-Einstein relation with the $[Fe(OH_2)_6]^{2/3+}$ radius $r = 2.060$ Å taken from R. L. Martin, P. J. Hay and L. R. Pratt, *J. Phys. Chem. A*, 1998, **102**, 3565, the diffusion coefficient (D°) is almost 1×10^{-9} m^2 s^{-1} for a single iron complex as compared to $D \sim 5.3 \times 10^{-9}$ m^2 s^{-1} for OH^- and $D \sim 9.31 \times 10^{-9}$ m^2 for H^+ at 25 °C in diluted solutions.
20 E. L. Cussler, *Diffusion Mass Transfer in Fluid Systems*, Cambridge University Press, Cambridge, 2nd edn, 1997, p. 143.
21 The expression of the effective diffusion coefficient D_{eff} in a cylindrical tube undergoing a Poiseuille flow is given by Taylor and Aris equation: $D_{eff} = D^\circ + \beta U^2 r^2/D^\circ$ where $\beta = 1/48$, U is the area-averaged mean flow velocity, r is the radius of the tube and D° is the molecule diffusivity in an unbounded fluid, see R. Aris, *Proc. R. Soc. London, Ser. A*, 1956, **235**, 67; G. I. Taylor, *Proc. R. Soc. London, Ser. A*, 1956, **219**, 186.
22 G. Mériguet, E. Dubois and R. Perzynski, *J. Colloid Interface Sci.*, 2003, **267**, 78.
23 F. Gazeau, E. Dubois, M. Hennion, R. Perzynski and Y. Raikher, *Europhys. Lett.*, 1997, **40**, 575.